ELSEVIER

Short communication

Imidazolium-organic solvent mixtures as electrolytes for lithium batteries

A. Chagnes [a], M. Diaw [b], B. Carré [a], P. Willmann [b], D. Lemordant [a, *]

[a] *Laboratoire de Physicochimie des Interfaces et Milieux Réactionnels (EA2098), Université de Tours, Faculté des Sciences et Techniques, Parc de Grandmont, F 37200 Tours, France*
[b] *Université Cheikh Anta Diop, Dakar, Sénégal*
[c] *CNES, 18 Avenue E. Belin, 31055 Toulouse Cedex, France*

Abstract

γ-Butyrolactone (BL) has been mixed to the room temperature ionic liquid (RTIL) 1-butyl 3-methyl-imidazolium tetrafluoroborate (BMIBF$_4$) (ratio: 3/2, v/v) in the presence of lithium tetrafluoroborate (LiBF$_4$) for use as electrolyte in lithium-ion batteries. This mixture exhibits a larger thermal stability than the reference electrolyte EC/DEC/DMC (2/2/1) + LiPF$_6$ (1 M) and can be considered as a new RTIL as no free BL molecules are present in the liquid phase. The cycling ability of this electrolyte has been investigated at a graphite, a titanate oxide (Li$_4$Ti$_5$O$_{12}$) and a cobalt oxide (Li$_x$CoO$_2$) electrodes. The ionic liquid is strongly reduced at the graphite electrode near 1 V and leads to the formation of a blocking film, which prevents any further cycling. The titanate oxide electrode can be cycled with a high capacity without any significant fading. Cycling of the positive cobalt oxide electrode was unsuccessfully owing to an oxidation reaction at the electrode surface, which prevents the intercalation or de-intercalation of Li ions in and from the host material. Less reactive cathode material than cobalt oxide must be employed with this RTIL.
© 2005 Elsevier B.V. All rights reserved.

Keywords: Electrolyte; Imidazolium; Ionic liquid; Lithium; Battery

1. Introduction

Investigations in the field of electrolyte for Lithium-ion batteries have seen tremendous increase in popularity. Despite the improvement and developments in safety of the lithium-ion batteries (shutdown separator [1,2], chemical shuttles [3,4], cathode additives [1,5], etc.), there are still safety problems concerning ignition or gas-built due to the low thermal stability, the high vapour pressure and the low flash point of these electrolytes. Actually most industrial electrolytes are mixtures of ethylenecarbonate (EC), diethylcarbonate (DEC) and dimethylcarbonate (DMC) with lithium hexafluorophosphate (LiPF$_6$) as salt. This type of electrolyte permits a great number of charge–discharge cycles without

noticeable loss in capacity but the search of new electrolytes with a high thermal stability is of great importance [6–16].

Room temperature ionic liquids (RTIL) can be potentially used as safe electrolytes in electrochemical applications owing to their wide thermal stability, wide liquid-phase range, non-flammability and very low vapour pressure [17,18]. These RTIL are composed of a cation like quaternary ammonium [19], alkylpyridinium [20], alkylpyrrolidinium [21], alkylpyrazolium [22], alkyltriazolium [23], alkylphosphonium [24] and alkylimidazolium [25], combined with a variety of large anions having a delocalized charge (PF$_6^-$, BF$_4^-$ and (Tf$_2$)N$^-$). All RTILs exhibit a high viscosity and, hence a relatively low conductivity. In order to decrease the viscosity and increase the conductivity, aprotic dipolar organic solvent may be added to RTIL. In these mixtures, as the organic solvent molecules solvate the ions of the RTIL inasmuch the solvent molecules are not

in excess as compared to the salt [26], the vapour pressure remains low and consequently the flash point remains high.

γ-Butyrolactone (BL) is an organic solvent with a high flash point, high boiling point, low vapour pressure, and moderate viscosity [26,28–30]. This organic solvent has been mixed to 1-butyl 3-methyl-imidazolium tetrafluoroborate (BMIBF$_4$) as RTIL in presence of lithium tetrafluoroborate (LiBF$_4$).

The composition of the γ-butyrolactone/BMIBF$_4$ mixture in presence of LiBF$_4$ has been optimized in term of conductivity as reported elsewhere [31]. The most conductive binary mixture contains 60% of BL and 40% of BMIBF$_4$ in volume.

The thermal stability of the electrolyte BMIBF$_4$/BL (40/60) + LiBF$_4$ (1M), referred as mixed RTIL electrolyte in the following has first been considered for potential use in lithium batteries. Thereafter, the cycling behaviour of this electrolyte has been investigated at a graphite, a Li$_4$Ti$_5$O$_{12}$ and a Li$_x$CoO$_2$ electrodes and compared to the reference electrolyte (EC/DEC/DMC (2/2/1) + LiPF$_6$ (1M)).

2. Experimental

BL (purity > 99.99%) was obtained from Aldrich and used as received. LiBF$_4$ (99.99%) was purchased by Fluka. BMIBF$_4$ (purity > 99.9%) was obtained by Aldrich and traces of moisture were eliminated in a Büchi vessel maintained at 60 °C under reduced pressure for 8 h. Electrolyte solutions were prepared by weight in a dry box. The reference electrolyte EC/DEC/DMC (2/2/1) + LiPF$_6$ (1M) was purchased from Merck (Selectipur®) and the water content of the solvents was less than 20 ppm as indicated by the manufacturer.

Differential scanning calorimeter (DSC) thermogramms were carried out at 10 K min^{-1} from 20 to 300 °C in 50 µL aluminium pans containing a small volume of electrolyte (10–20 µL). The pans were not hermetically sealed but the cover were holed to permit the evacuation of the gas produced by the thermal decomposition of the electrolyte. The reference cell was an aluminium pan filled with silica powder.

The graphite electrodes, a mixture of rhombohedral and hexagonal graphites, were kindly provided by SAFT as well as the lithiated titanate (Li$_4$Ti$_5$O$_{12}$) and cobalt (Li$_x$CoO$_2$) electrodes. Graphite/Li, Li$_4$Ti$_5$O$_{12}$/Li and Li$_x$CoO$_2$/Li half-cells were built using Swagelock connectors and cycled with an Arbin battery cycler. Charge and discharge of half-cells were operated in a galvanostatic mode at a C/15 rate (a C/15 rate corresponds to a current density at which the full capacity of the material can be charged (or discharged) in 15 h). All potentials were referred to the Li$^+$/Li system. For cycling ability experiments, graphite/Li and Li$_4$Ti$_5$O$_{12}$ half-cells were charged at constant current to a low cut-off voltage of, respectively, −0.01 V and +1.1 V. The Li$_x$CoO$_2$/Li half-cell was charged up to +4.3 V. Discharge was operated at the same constant current, to a cut-off voltage of +2.5 V for graphite/Li, +2.3 V for Li$_4$Ti$_5$O$_{12}$/Li and +3.5 V for Li$_x$CoO$_2$/Li. Cyclic voltammogramms were obtained at a 0.1 mV s^{-1} scan rate between −20 mV and +2.5 V for the graphite electrode and between +1.1 and +1.9 V for the Li$_4$Ti$_5$O$_{12}$ electrode. Linear sweep voltammetries were carried out at 0.1 mV s^{-1} between +3 and +5.5 V at a Li$_x$CoO$_2$ composite electrode.

3. Results and discussions

Addition of BL to BMIBF$_4$ decreases drastically the viscosity from 217 cP for BMIBF$_4$ + LiBF$_4$ (1 M) to 10.5 cP for the mixed RTIL electrolyte at 25 °C. Simultaneously, the conductivity increases from 2.5 mS cm^{-1} for BMIBF$_4$ + LiBF$_4$ (1 M) to 9.5 mS cm^{-1} for the mixed RTIL electrolyte at 25 °C [31].
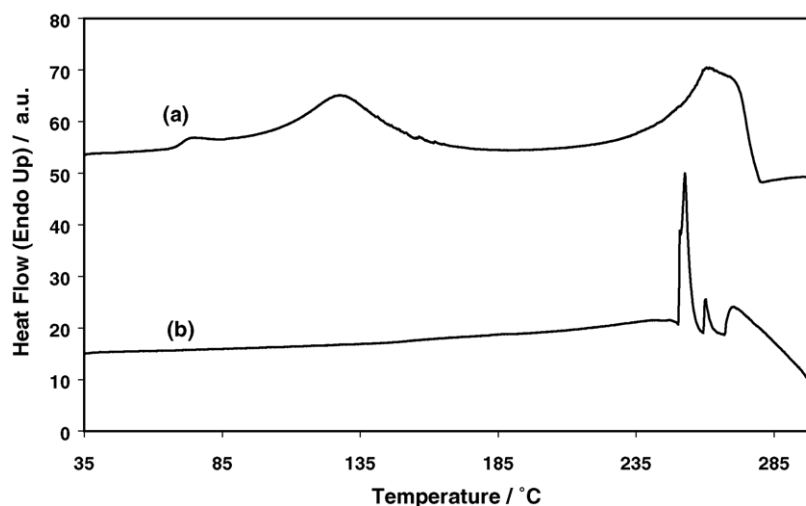

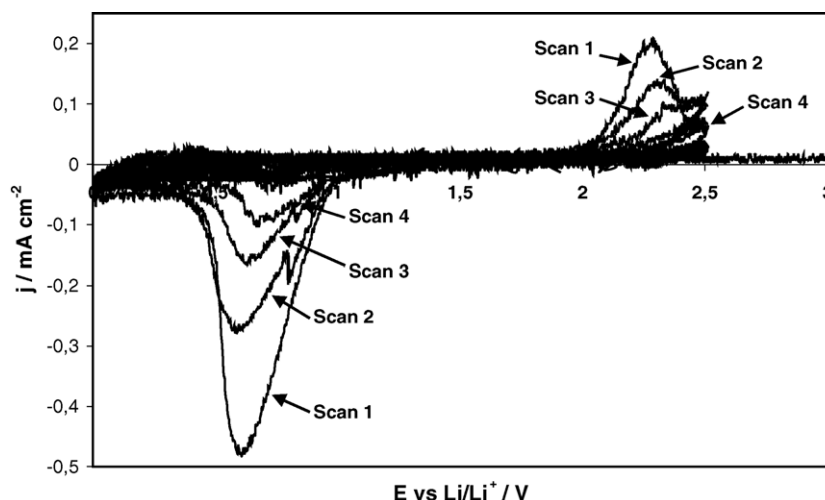Fig. 1. DSC thermogramm of (a) EC/DEC/DMC (2/2/1) + LiPF$_6$ (1 M) and (b) the mixed RTIL electrolyte at a rate of 10 °C min^{-1}.

Fig. 2. Cyclic voltamperometry ($0.1\,mV\,s^{-1}$) of the mixed RTIL electrolyte at a graphite electrode.

3.1. Thermal stability

DSC thermogramms of the EC/DEC/DMC reference electrolyte and the mixed RTIL electrolyte are reported in Fig. 1a. The thermogram of the reference electrolyte, reported in Fig. 1a, displays three endothermic peaks. The onset of these peaks are, respectively, at 69, 105 and 225 °C and may be compared to the boiling temperature of the pure solvents at the atmospheric pressure: 90 °C (DMC), 127 °C (DEC) and 243 °C (EC) [32]. The last endothermic peak is followed by an exothermic reaction, which may correspond to the reaction of $LiPF_6$ or some of its decomposition products (HF, PF_5, . . .) with the aluminium pan [18].

The thermogram of the mixed RTIL electrolyte (Fig. 1b) shows a greater thermal stability range than the reference electrolyte as no peak is observed below 248 °C. Between 248 and 283 °C, the thermogram exhibits three endothermic peaks, which are followed by an exothermic reaction above 283 °C. As no decomposition of the RTIL occurs be-

low 320 °C [27] and as BL has a boiling point of 207 °C at the atmospheric pressure [32], it is inferred that the endothermic peaks correspond, at least partially to the vaporization of strongly solvated BL molecules. This experiment reveals the enhanced stability of organic solvents like BL when mixed with a very stable RTIL. The exothermic peak may correspond to a reaction of the aluminium pan with decomposition products of the salt ($LiBF_4$) [18]. The mixed RTIL electrolyte is far more thermally stable than the reference electrolyte.

3.2. Electrochemical behaviour of the mixed RTIL electrolyte at the graphite electrode

Fig. 2 displays the successive cyclic voltammogramms obtained at a graphite electrode in a half-cell. Reduction of the electrolyte begins at 1 V with a maximum peak located at 0.6 V (first scan). No lithium deposition or insertion occurs till −0.02 V. On the reverse scan, an oxidation peak is observed at 2 V (maximum at 2.3 V). This peak corresponds to
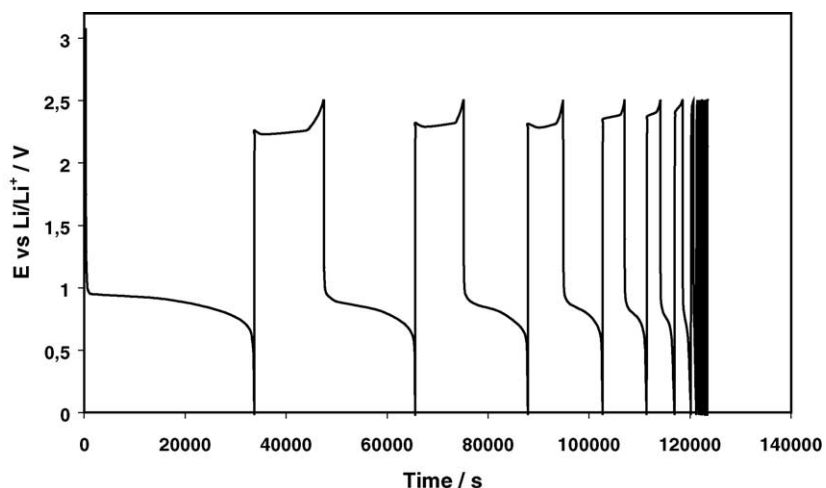

Fig. 3. Cycling ability of the mixed RTIL electrolyte at a graphite electrode; 15 h per charge or discharge (C/15).

the oxidation of the products obtained at the electrode during the reduction scan, as no peaks are observed if the reverse potential is fixed at 1 V or more. The area under the reduction and oxidation peaks decreases progressively during the following scans, which means that the reduction products of the electrolyte precipitates onto the graphite surface to form a solid film. This film may be partially re-dissolved during the reverse scan. After the fifth cycle, the film onto the graphite electrode remains stable and no dissolution occurs as evidenced by the absence of reduction and oxidation peaks.

The result of the galvanostatic chronopotentiometry at the graphite electrode is reported in Fig. 3. During the charge cycle, the potential of the cell remains constant at 1 V, in accordance, which has been stated before. During the discharge, the potential is maintained at 2.5 V with which correspond to the re-oxidation of the deposited film. As expected no Li insertion occurs during the cycling owing to the reduction of the electrolyte, which forms an isolating film at the electrode surface.

As a conclusion, the graphite electrode cannot be cycled in the investigated electrolyte. As the reduction of the electrolyte occurs near 1 V, the graphite electrode may be advantageously replaced by a $Li_4Ti_5O_{12}$ electrode.

3.3. Electrochemical behaviour of the mixed RTIL electrolyte at the $Li_4Ti_5O_{12}$ electrode

According to the following equation:

$$Li_4Ti_5O_{12} + 3Li^+ + 3e^- \rightarrow Li_7Ti_5O_{12}$$
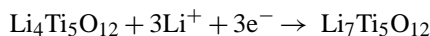
the $Li_4Ti_5O_{12}$ electrode allows insertion at 1.55 V with a theoretical capacity of 175 mAh g^{-1} [33]. It has been found experimentally that this electrode has a capacity close to the theoretical capacity of 175 mAh g^{-1} [33–36] at the first cycle and 150 mAh g^{-1} after a couple of charge–discharge cycles, which remains stable for at least 100 cycles [35,37].

The cycling ability of the $Li_4Ti_5O_{12}$ electrode has been tested at a charge rate of C/15 with the EC/DEC/DMC reference electrolyte and the mixed RTIL electrolyte. Insertion and de-insertion of lithium ions from the host material in EC/DEC/DMC reference electrolyte are perfectly reversible as the charging and discharging capacities are equal and decrease slowly from 157 to 143 mAh g^{-1}. A loss of 9% of the initial capacity occurs during the 19 first cycles.

In Fig. 4 are displayed two successive cyclic voltammogramm curves obtained at a $Li_4Ti_5O_{12}$ electrode for a scan rate of 0.1 mV s^{-1}. The cycles are reproducible and the peaks exhibit symmetrical shapes with a fast and highly reversible lithium acceptance–removal process in the electrode material.

Cycling ability tests have been performed in order to investigate the lithium insertion and de-insertion over 19 cycles (Fig. 5). It shows that the insertion plateau potential occurs at 1.55 V and the de-insertion plateau is located at 1.6 V, independently of the cycle number. Charge and discharge potentials are different owing to the IR drop in the cell. The cycling capacities, determined by galvanostatic chronopotentiometry

during 19 cycles at C/15, are reported in Fig. 6. As charge capacities are practically equal to discharge capacities, only the mean value has been reported. The charge capacities of the $Li_4Ti_5O_{12}$ electrode in the two electrolytes are similar but a slightly lower loss in capacity is observed when the reference electrolyte is employed (9% instead of 11%). This cycling test demonstrates that the $Li_4Ti_5O_{12}$ electrode can be used as a negative electrode in the mixed RTIL electrolyte.

3.4. Electrochemical behaviour of the mixed RTIL electrolyte at the Li_xCoO_2 electrode

The Li_xCoO_2 electrode may be used as a high potential positive electrode. In the reference electrolyte, linear sweep voltamograms at the Li_xCoO_2 electrode are characterized by three successive oxidation peaks. The first peak at 3.9 V is associated to the de-intercalation of Li ions according to [38]:

$$LiCoO_2 \rightarrow Li_{1-x}CoO_2 + xLi^+ + xe^-$$

and the two following peaks, between 4.2 and 4.8 V, are attributed to phase transition occurring in the electrode material.

Fig. 7 displays a linear sweep voltammogramm and a galvanostatic chronopotentiogramm obtained at a Li_xCoO_2 electrode in presence of the mixed RTIL electrolyte. As seen in Fig. 7a, an oxidation wave starts at 3.8 V followed by a strong raise in current density at 4.2 V. Li_xCoO_2 cathodes are usually used with conventional electrolytes such as alkycarbonate-based electrolytes in presence of LiPF$_6$ and electrochemical window of these electrolytes permits charge–discharge cycles with Li_xCoO_2 electrode. The electrochemical stability of an electrolyte depends on the composition of the electrolyte and the nature of the electrode material. In fact, the electrochemical stability of the investigated electrolyte is equal to 5.5 V at 5 mV s^{-1} [31] when a platinum electrode is used instead of a cobalt electrode. The raise in current at 3.8 V may be attributed to a catalytic effect of the Li_xCoO_2 surface, which may favorize the oxidation of the imidazolium-based electrolyte.

In Fig. 7b, a plateau is observed at 3.95 V and corresponds to the potential when an increase of the current is observed in Fig. 7a by linear voltammetry. This potential corresponds to the oxidation of the electrolyte. The potential remains constant for a C/15 rate during at least 4 days. It is inferred from this experiment that the electrolyte is oxidized at this potential and that this electrode cannot be used as a positive electrode in the mixed RTIL electrolyte. As the oxidation potential of the electrolyte is close to the potential of de-intercalation of the Li ions from this electrode, the search of a positive electrode having a lower de-intercalation potential is required. Li_xFePO_4 is a promising cathode material when the electrolyte has a low electrochemical stability because its operating voltage is lower than traditional cathode such as Li_xCoO_2 or Li_xNiO_2 (3.5 V versus Li or 2 V versus $Li_4Ti_5O_{12}$) [39] and this operating voltage is lower than the oxidation potential of the investigated electrolyte.
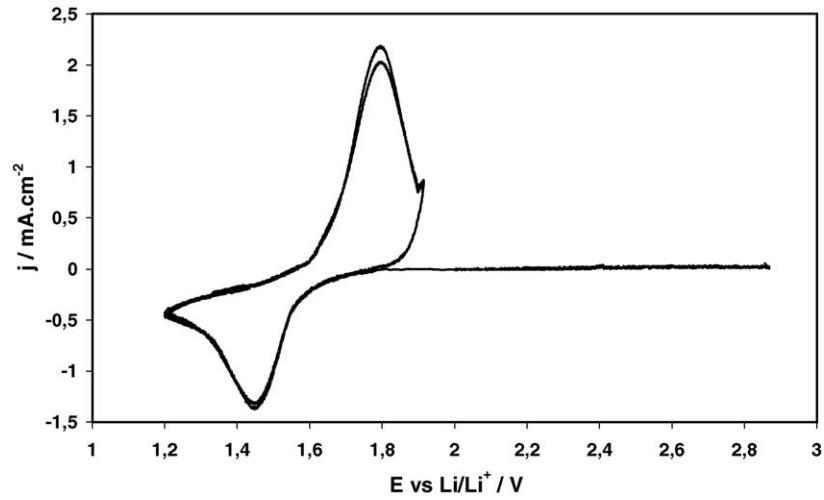
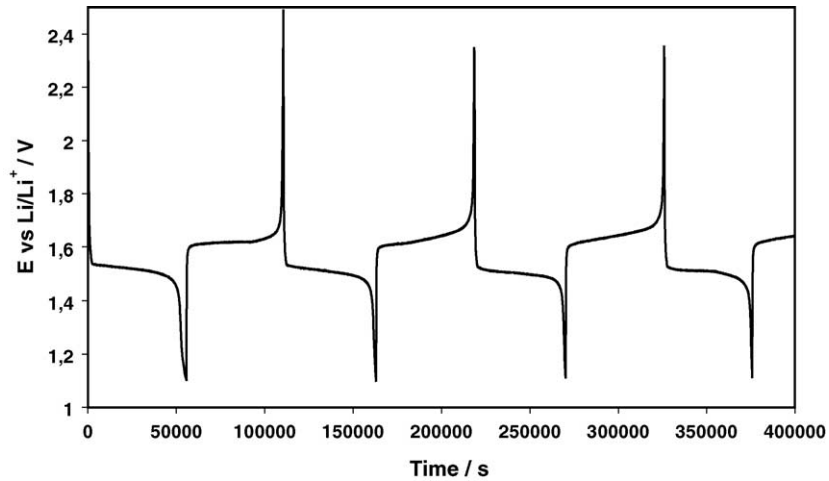Fig. 4. Linear sweep voltammetry (0.1 mV s^{-1}) of the mixed RTIL electrolyte at a Li$_4$Ti$_5$O$_{12}$ composite electrode.

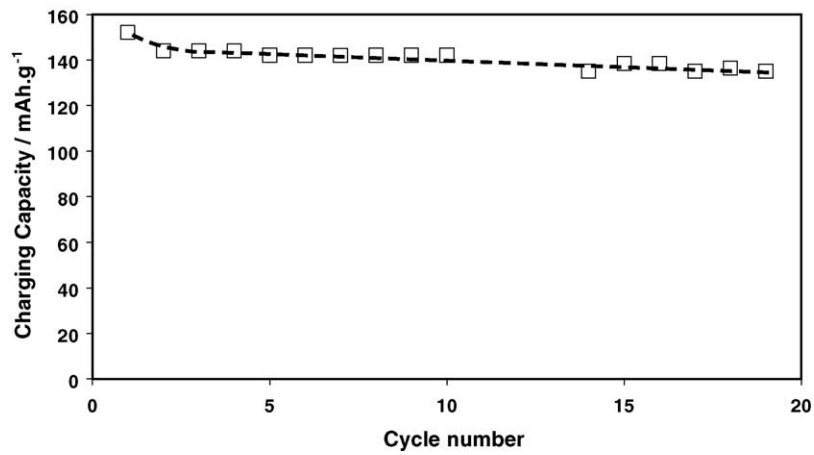Fig. 5. Cycling ability of the mixed RTIL electrolyte at a Li$_4$Ti$_5$O$_{12}$ composite electrode (C/15).

Fig. 6. Charging capacity vs. cycle number during cycling ability test of the mixed RTIL electrolyte at a Li$_4$Ti$_5$O$_{12}$ composite electrode (C/15).

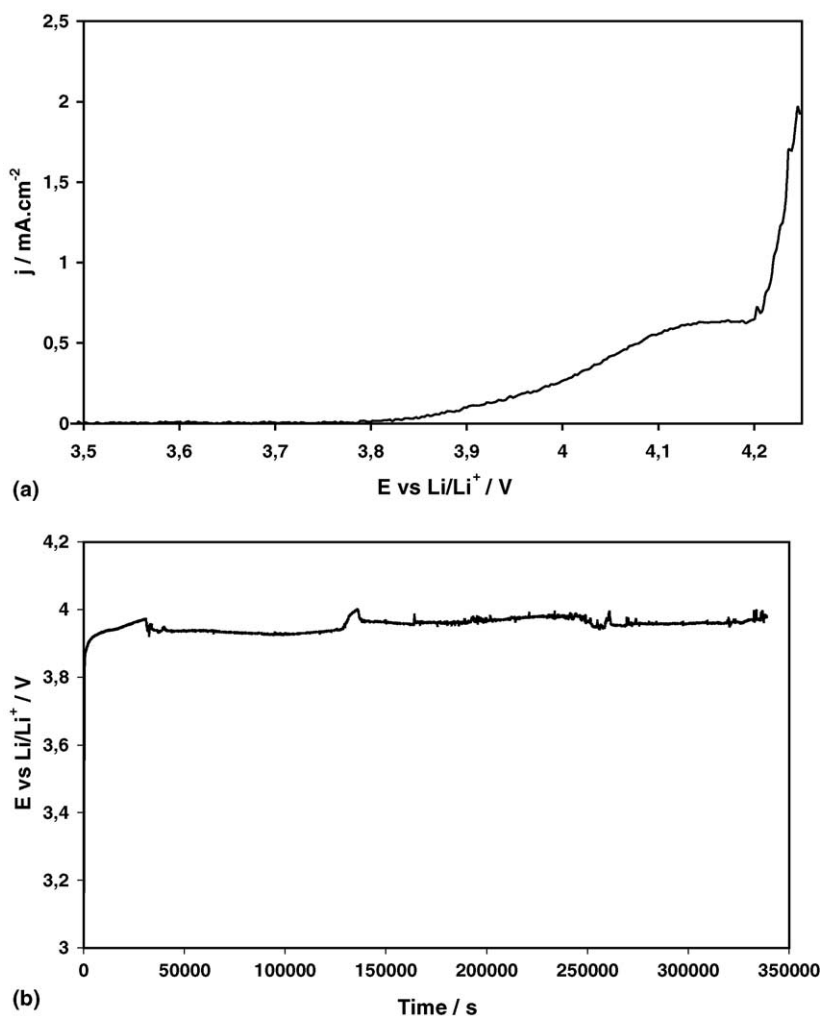Fig. 7. (a) Linear sweep voltammetry (0.1 mV s^{-1}) of the mixed RTIL electrolyte at a Li$_x$CoO$_2$ composite electrode. (b) Cycling ability test at a Li$_x$CoO$_2$ composite electrode in presence of the mixed RTIL electrolyte (C/15).

4. Conclusion

Mixtures of 1-butyl 3-methyl-imidazolium tetrafluoroborate with γ-butyrolactone in presence of lithium tetrafluoroborate exhibit a better thermal stability than the reference electrolyte EC/DEC/DMC (LiPF$_6$, 1 M) at high temperature as no solvent evaporation occurs owing to the strong ion–dipole interactions between the imidazolium cation and BL molecules. A conductivity greater than the reference electrolyte is achieved at room temperature. In order to use this electrolyte in lithium batteries, a titanate electrode (Li$_4$Ti$_5$O$_{12}$) has been used instead of the more common graphite electrode as the ionic liquid is responsible of a high resistivity of the SEI film. No significant fading during the following cycles is observed when Li$_4$Ti$_5$O$_{12}$ is used as a negative electrode. The cycling ability of a Li$_x$CoO$_2$ positive electrode has also been investigated but unsuccessfully owing to the oxidation of the ionic liquid at the electrode surface. Future works will concern the search of alternative positive electrodes such as Li$_x$FePO$_4$ and the use of additive,

like vinylene carbonate (VC) to improve the quality and the stability of the SEI layer of the graphite electrode. Investigations are in progress to prepare Li$_x$FePO$_4$ materials in order to investigate as soon as possible the electrochemical behaviour of this material in presence of ionic liquid-based electrolytes.

References

[1] K. Ozawa, Solid State Ionics 69 (1994) 212.
[2] F.C. Laman, M.A. Gee, J. Denovan, J. Electrochem. Soc. 140 (1993) L51.
[3] M.N. Golovin, D.P. Wilkinson, J.T. Dudley, D. Holonko, S. Woo, J. Electrochem. Soc. 139 (1992) 5.
[4] T.J. Richardson, P.N. Ross, J. Electrochem. Soc. 143 (1996) 3992.
[5] U. von Sacken, Paper presented at POWER'97, Proceedings of the 5th International Conference on Power Requirements for Mobile Computing and Wireless Communications, Santa Clara, CA, October 12–15, 1997.
[6] G.G. Botte, R.E. White, Z. Zhang, J. Power Sources 97–98 (2001) 570.
[7] Z. Zhang, D. Fouchard, J.R. Rea, J. Power Sources 70 (1998) 16.

[8] U. von Sacken, E. Nodwell, A. Sundher, J.R. Dahn, Solid State Ionics 69 (1994) 284.

[9] J.R. Dahn, E.W. Fuller, M. Obravae, U. von Sacken, Solid State Ionics 69 (1994) 265.

[10] A. Du Pasquier, F. Disma, T. Bowmer, A.S. Gozdz, G. Amatucci, J.M. Tarascon, J. Electrochem. Soc. 145 (1998) 472.

[11] M.A. Gee, F.C. Laman, J. Electrochem. Soc. 140 (1993) L53.

[12] J.-S. Hong, H. Maleki, S. Al Hallaj, L. Redey, J.R. Selman, J. Electrochem. Soc. 145 (1998) 1489.

[13] M.N. Richard, J.R. Dahn, J. Electrochem. Soc. 146 (1999) 2068.

[14] A. Ohta, H. Koshina, H. Okuno, H. Murai, J. Power Sources 54 (1995) 6.

[15] E.P. Roth, Abstract 388, in: The Electrochemical Society Meeting Abstracts, vol. 99-2, Honolulu, HI, October 17–22, 1999.

[16] K. Kumai, H. Miyashiro, Y. Kobayashi, K. Takei, R. Ishikawa, J. Power Sources 81–82 (1999) 715.

[17] Y. Hu, H. Li, X. Huang, L. Chen, Electrochem. Commun. 6 (2004) 28.

[18] H.L. Ngo, K. LeCompte, L. Hargens, A.B. McEwen, Thermochim. Acta 357–358 (2000) 97.

[19] J. Sun, M. Forsyth, D.R. MacFarlane, J. Phys. Chem. B 102 (1998) 8858.

[20] H.L. Chum, R.A. Osteryoung, in: D. Inman, D. Lovering (Eds.), Ionic Liquids, Plenum Press, New York, 1981.

[21] D.R. MacFarlane, P. Meakin, J. Sun, N. Amini, M. Forsyth, J. Phys. Chem. B 103 (1999) 4164.

[22] J. Caja, T.D.J. Dunstan, D.M. Ryan, V. Katovic, The Electrochemical Society and The Electrochmical Society of Japan Meeting Abstracts, vol. 99-2, 1999, p. 2252.

[23] B. Vestergaard, N.J. Bjerum, I. Petrushina, H.A. Hjuler, R.W. Gerg, M. Begtrup, J. Electrochem. Soc. 140 (1993) 3108.

[24] J.D. Holbery, K.R. Seddon, Clean Products Process 1 (1999) 223.

[25] L.A. Blanchard, D. Hancu, E.J. Beckman, J.F. Brennecke, Nature 99 (1999) 28.

[26] A. Chagnes, B. Carré, P. Willmann, D. Lemordant, Electrochim. Acta 46 (2001) 1783.

[27] A. Chagnes, B. Carré, H. Allouchi, B. Carré, D. Lemordant, Solid State Ionics, submitted for publication.

[28] A. Chagnes, B. Carré, P. Willmann, D. Lemordant, J. Power Sources 109 (2002) 203.

[29] A. Chagnes, H. Allouchi, B. Carré, G. Odou, P. Willmann, D. Lemordant, J. Appl. Electrochem. 33 (2003) 589.

[30] A. Chagnes, B. Carré, P. Willmann, R. Dedryvère, D. Gonbeau, D. Lemordant, J. Electrochem. Soc. 150 (9) (2003) A1255.

[31] M. Diaw, A. Chagnes, B. Carré, P. Willmann, D. Lemordant, J. Power Sources, ILMB 12, in press (Special issue).

[32] M. Wakihara, in: O. Yamamoto (Ed.), Lithium Ion Batteries Fundamentals and Performance, Wiley-VCH, Berlin, 1998.

[33] S.I. Pyun, S.W. Kim, H.C. Shin, J. Power Sources 81–82 (1999) 248.

[34] K.M. Colbow, J.R. Dahn, R.R. Haering, J. Power Sources 26 (1989) 397.

[35] C.H. Chen, J.T. Vaughey, A.N. Jansen, D.W. Dees, A.J. Kahaian, T. Goacher, M.M. Thackeray, J. Electrochem. Soc. 148 (2001) A102.

[36] K. Zaghib, M. Armand, M. Gaulthier, J. Electrochem. Soc. 145 (1998) 3135.

[37] T. Ohzuku, A. Ueda, N. Yamamoto, J. Electrochem. Soc. 142 (1995) 1431.

[38] I. Geoffroy, A. Chagnes, B. Carré, D. Lemordant, P. Biensan, S. Herreyre, J. Power Sources 112 (2003) 191.

[39] K. Striebel, A. Guerfi, J. Shim, M. Armand, M. Gauthier, K. Zhaghib, J. Power Sources 119–121 (2003) 951–954.